CMAQ NUCLEATION ALGORITHMS AND THEIR IMPACT ON PM MODELING RESULTS IN THE LOWER FRASER VALLEY

Helmut Roth *, Weimin Jiang, Dazhong Yin, and Éric Giroux
ICPET, National Research Council of Canada, Ottawa, On, Canada
e-mail: helmut.roth@nrc-cnrc.gc.ca
Voice (613) 993-7731 Fax (613) 941-1571

1. INTRODUCTION

CMAQ offers the user a number of options for modeling various processes, but it may not always be clear when one option is preferable to another, what the differences are between the various options, what the effects of these differences are on concentration fields, etc. In this study, we look at the number and mass production rates of three aerosol nucleation algorithms available in various versions of CMAQ, and the resulting influence of the algorithms on the concentrations of aerosol particle number and sulfate mass during a simulation of the Pacific '93 pollution episode in the Lower Fraser Valley.

In CMAQ, aerosol size distribution is modeled as a superposition of three lognormal distribution functions, or modes, each characterized by a geometric mean diameter and geometric standard deviation. The three distributions are referred to as the Aitken or i mode, the accumulation or j mode, and the coarse or c mode. Aerosol species in CMAQ belong to a particular mode. Thus aerosol sulfate appears as the two model species ASO4I (i-mode) and ASO4J (j-mode).

Nucleation in CMAQ is based on a binary model involving gas-phase water and sulfuric acid. The new particle production rate depends on relative humidity, temperature, and sulfuric acid vapour source rate, which is the concentration of the pseudo gas-phase precursor species SULAER divided by the length of the time step. All of the SULAER (H_2SO_4 vapour from chemical reactions) produced in a time step is transferred to particulate matter by nucleation and condensation. The nucleated mass goes to ASO4I, whereas the condensed mass is split between ASO4I and ASO4J.

* *Corresponding author address:* Helmut Roth, ICPET, National Research Council of Canada, 1200 Montreal Road, Ottawa, On, Canada K1A 0R6.

2. THE NUCLEATION ALGORITHMS

One nucleation algorithm, hereafter referred to as HK98, is an implementation of the Harrington and Kreidenweis (1998) parameterization. Briefly, this parameterization is based on solutions of the fully coupled dynamics equations of a two mode, two moment model. HK98 is available in the CMAQ *aero2* aerosol module.

Both of the other algorithms are implementations of the parameterization of Kulmala et al (1998), which is based on solutions to the equations of classical nucleation theory. The first, which we call KLP2, is available in the *aero2* module, and the second, KLP3, is available in *aero3*. KLP2 and KLP3 are very similar, and we occasionally use KLPx to refer to both. They differ primarily in the size distribution and mass of new particles. These details can be found in the source code and are described in Jiang and Roth (2003).

3. MODELING DOMAINS AND INPUTS

Figure 1 shows the two nested horizontal grid domains (left) used in the CMAQ modeling. They are defined on a Lambert Conformal projection with origin at 123°W, 49.15978°N. Secant angles are 48.75°N and 49.50°N. The outer domain contains 25×44 grid cells of size 15km × 15km each. The inner domain (right) consists of 33×30 grid cells of 5km × 5km each. It contains the Lower Fraser Valley region, including Vancouver and its suburban areas in Canada along with Bellingham and Burlington in the US.

Vertically, there are 15 terrain-following layers defined by σ values at the layer boundaries. The pressure at the top of the highest layer is 10 kpa.

Meteorological input for CMAQ was obtained from an MM5 simulation (Yin et al 2002) for the Pacific '93 pollution episode (Steyn et al 1997).

Emissions input, comprised of area, biogenic, mobile and point sources, was prepared with SMOKE (Giroux et al 2003). Daily emission inventories for the episode (Levelton 1995) were included in the modeling.

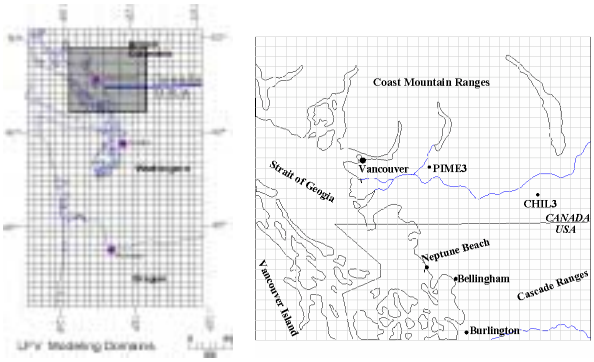

Fig. 1 Nested domains (left) and inner domain detail (right).

4.0 Nucleation Rates

We modified the *aero2* source code, making it modular at the process level, allowing us to easily turn aerosol processes on or off (Jiang and Roth 2002). We also arranged to track SULAER concentrations and timestep length dt. Further modifications allowed us to read gas-phase concentrations from a CMAQ output file and use those for input to the modified *aero2* module.

A nested domain run with no aerosol processes at all (using module *aero_noop*) provided the same gas-phase concentrations for each of three subsequent inner domain simulations. These three runs differed only in the choice of nucleation algorithm, with all other aerosol processes switched off. At each hour, the aerosol module used the gas-phase data to make nucleation rate calculations for one timestep of length dt. We imposed a minimum new particle rate of 1 m^{-3} s^{-1}.

4.1 Results

Figure 2 shows the evolution of domain-averaged first layer i-mode particle number production rate from the three algorithms, along with the domain-averaged input SULAER concentration. The corresponding mass production rates (not shown) showed a similar pattern. Because the nucleated particles are very small, mass nucleation rate is also small.

SULAER concentration and the nucleation rates both show a diurnal pattern with early afternoon peaks, though the rates from KLPx are often minimum. The number rate for HK98 closely follows the SULAER pattern and is typically four or five orders of magnitude greater than the KLPx rates. However, on August 5 and 7 the KLPx rates rise to roughly 40% of the HK98 rate, so that on an episode-average basis the HK98 rate is about eight times that of KLPx.

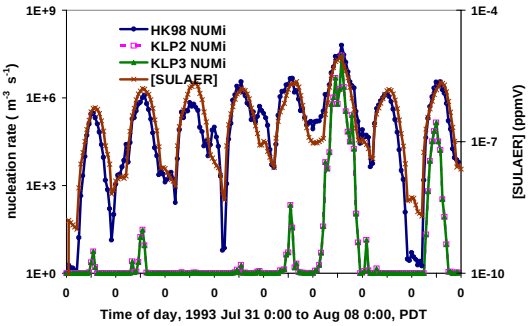

Fig. 2. Eight day time series of spatially averaged 1st layer mean number nucleation rate and available SULAER concentration.

Table 1 reports first layer peak number production rates (m^{-3} s^{-1}) in the episode from the three nucleation algorithms. Maximum production by cell and by domain-average are both shown, as is the average production rate for the entire episode. The three algorithms are consistent with respect to time and place of maximum nucleation rate. In all cases peak production occurs in the early afternoon of August 5, at 13:00 by cell value and one hour later by domain average. All cell maxima occurred in cell (17,8), location of Neptune Beach, about 10 km northwest of Bellingham, Wa. This cell has the highest sulfate emission rate throughout the episode, providing a relatively high H_2SO_4 vapour source rate for nucleation.

Method	*Peak cell*	*Peak spatial mean*	*Episode average*
HK98	5.15e09	6.30e07	16.20e05
KLP2	10.95e09	2.82e07	2.12e05
KLP2	10.95e09	2.82e07	2.12e05

Table 1 Comparison of first layer number production rates (m^{-3} s^{-1}), by peak cell value, peak spatial mean, and whole episode average.

Although the maximum rate in a cell is greater from the KLP algorithms (roughly double that from HK98), the domain-averaged number production rate from HK98 is generally much greater than the rates from KLPx, and on an episode average basis, HK98 number production exceeds that of KLPx by a factor of nearly 8.

The algorithms show quite a different response to the ambient conditions encountered: HK98 rate followed the SULAER concentration pattern and almost always gave significant production, while KLP often offered only the imposed minimum rate. When the conditions favoured a response from the KLP algorithms, they sometimes gave greater production than HK98. On domain and episode average bases, however, HK98 showed greater production rates than the KLP algorithms.

Correlation between HK98 and KLPx was generally poor, but at the hour of peak average number nucleation rate there is a high degree of correlation among all the algorithms. Considering only cells with greater than minimum production, we find r^2 = 0.91 between HK98 and KLPx (0.87 with all cells), and r^2 = 1.0 between KLP2 and KLP3.

5.0 Impact on i-mode number and sulfate concentration

To assess the impact of the nucleation algorithms on CMAQ PM modeling results, we ran one outer domain and four inner domain simulations. Here all aerosol processes were switched on, and the HK98 algorithm (default in *aero2*) was used for nucleation in the outer domain.

Output from the outer domain provided initial and boundary data for the inner domain. One of the inner domain runs, referred to below as Noop, had nucleation switched off, while the other three differed only in the choice of nucleation algorithm. All other aerosol processes were switched on, and all runs did full gas-phase calculations.

5.1 Number and sulfate mass concentrations

Time series of the first layer spatially averaged concentrations for total i-mode number and sulfate mass (ASO4I) are shown in Figures 3 and 4. The KLP algorithm results closely follow those of no nucleation, within 1% for number and 2% for mass. Differences between KLP2 and KLP3 are not discernable. Response to HK98 is greater, with relative differences from Noop concentrations as high as 400% for number and 300% for mass. Over the episode, average HK98 i-mode number concentration exceeded that of Noop by 58%.

Figure 5 shows the spatial distribution of first layer temporally averaged i-mode number concentration

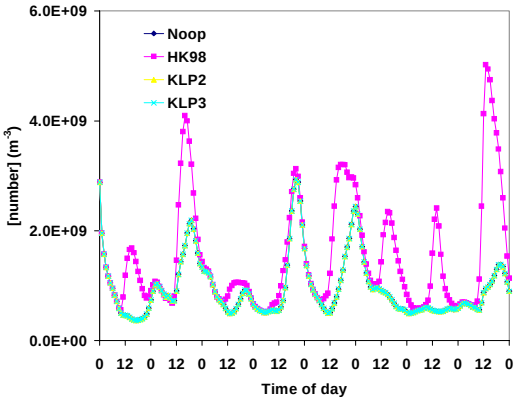

Fig. 3 Time series of spatially averaged first layer i-mode number concentration, 1993 Jul 31 0:00 to Aug 07 0:00, PDT.

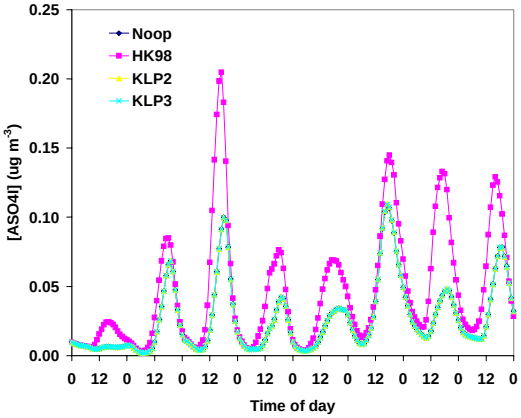

Fig. 4 Time series of spatially averaged first layer i-mode sulfate mass concentration, 1993 Jul 31 0:00 to Aug 08 0:00, PDT.

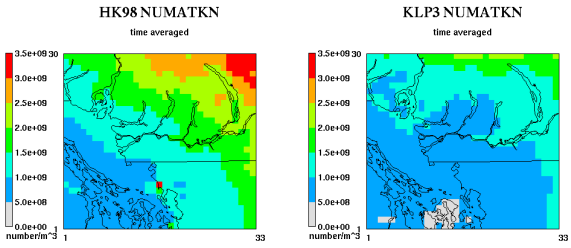

Fig. 5 Spatial distribution of time averaged 1st layer i-mode number concentration for HK98 (left) and KLP3 (right). KLP2 and Noop results are similar to KLP3.

from HK98 and KLP3. The distributions from KLP2 and Noop are virtually identical to KLP3 and not shown. Both distributions show a general SW to NE increase, but HK98 has a greater range, and shows a peak at Neptune Beach that is not shown by the other simulations.

We used the PMx software of Jiang and Yin (2001) to extract $PM_{2.5}$ concentration data from the CMAQ output data. Time series of spatially averaged first layer $PM_{2.5}$ number concentrations (not shown) have pattern similar to the i-mode number series in Figure 3, but with concentrations roughly 90% higher. Over the episode, HK98 increases first layer $PM_{2.5}$ number concentration by roughly 33% with respect to no nucleation.

None of the algorithms show much difference from Noop with respect to spatially averaged $PM_{2.5}$ sulfate mass. This is dominated by contributions from the j-mode, which overwhelm the signal from the i-mode. Furthermore, all of the reacted H_2SO_4 in a time step goes to i- and j-mode sulfate mass by nucleation and condensation. The total new mass is thus independent of the number of new particles, so results from all methods including Noop will be similar whenever $ASO4_{i+j}$ is a good approximation of $ASO4_{2.5}$.

6. CONCLUSIONS

- The KLP2 and KLP3 algorithms gave similar results
- The HK98 algorithm differed significantly from the KLP algorithms, particularly with respect to number production rate, impact on i-mode and $PM_{2.5}$ number concentration, and impact on i-mode mass concentration.
- Throughout the simulations, the HK98 algorithm showed higher domain-average number and mass production rates, but the KLP algorithms had the highest peak number production rate in a single cell.
- On an episode average basis, the HK98 algorithm increased number concentration by 58% in i-mode and 33% in $PM_{2.5}$, compared to no nucleation, but the KLP algorithms showed no difference.
- On a domain-average basis, none of the algorithms showed a substantial increase over no nucleation in $PM_{2.5}$ mass concentrations.
- Comparison with measured number concentration is still required to see which algorithm is most appropriate.

ACKNOWLEGEMENTS

This work was funded by the National Research Council of Canada and the Program on Energy Research and Development in Canada. Original CMAQ source code was obtained from the U.S. EPA.

REFERENCES

Giroux E., H. Roth, D. Yin and W. Jiang, 2003: Preparing emission input files using SMOKE for CMAQ applications in the Lower Fraser Valley, ICPET, National Research Council of Canada draft report.

Harrington, D. and S. Kreidenweis, 1998: Simulations of sulfate aerosol dynamics—I. Model description. *Atmos. Environ.* **32**:1691–1700.

Jiang, W. and D. Yin, 2001: Development and application of the PMx software package for converting CMAQ modal particulate matter results into size resolved quantities, National Research Council of Canada report number PET-1497-01S.

Jiang, W. and H. Roth, 2002: Development of a modularized aerosol module in CMAQ, *Extended Abstract, CMAS Models-3 users' workshop*, EPA, Research Triangle Park, NC, US EPA.

Jiang, W. and H. Roth, 2003: A detailed review and analysis of science, algorithms, and code in the aerosol components of Models-3/CMAQ I. Kinetic and thermodynamic processes in the aero2 module, National Research Council of Canada, report number PET-1534-03S, 118pp.

Kulmala, M., A. Laaksonen, and L. Pirjola, 1998: Parameterizations for sulphuric acid/water nucleation rates. *J. Geophys. Res*. **103**: 8301–8307.

Levelton Engineering Ltd., 1995: Pacific 93 Air Emissions Inventory Draft Report, Technical Report 495-195, Prepared for Science Division, Environmental Conservation Branch, Environment Canada, Pacific and Yukon Region, 80pp.

Steyn, D., J. Bottenheim, R.Thomson, 1997: Overview of Tropospheric Ozone in the Lower Fraser Valley, and the Pacific '93 Field Study, *Atmospheric Environment*, **31**, 2025-2035.

Yin, D., H. Roth and W. Jiang, 2002: Meteorological modeling using MM5 for the Pacific '93 air pollution episode in the Lower Fraser Valley, National Research Council of Canada, Ottawa, ON, report number PET-1530-02S, 74pp.